

Influence of magma composition and oxygen fugacity on the crystal structure of C2/c clinopyroxenes from a basalt-pantellerite suite

C. Carbonin¹, A. Dal Negro¹, S. Ganeo¹, and E.M. Piccirillo²

¹ Dipartimento di Mineralogia e Petrologia, Università di Padova, Corso Garibaldi 37, 35122 Padova, Italy

² Istituto di Mineralogia e Petrografia, Università di Trieste, Italy

Received July 5, 1990 / Accepted January 25, 1991

Abstract. The crystallochemical variations of clinopyroxene in response to changes in f_{O_2} and melt composition have been determined for a basalt-pantellerite suite (Bosetti Complex, Main Ethiopian Rift) by crystal structure refinement and microprobe analysis. The pyroxene evolutionary trend has both a “Ca-minimum” and late iron enrichment. During crystallization from basalts to trachytes, clinopyroxene geometry depends mainly on the relationships between T and M2 sites; for example, high SiO₂ activity in the magma causes high Si occupancy in T site, which in turn requires low Ca occupancy in M2 site in order to fulfill the local charge balance requirements. In contrast, clinopyroxene crystallized from acid melts is characterized by high Fe²⁺ (M1) content and therefore by a very large M1 site. Longer $\langle M1-O1 \rangle$ and $M1-O2$ bond lengths require shorter T–O1 and T–O2 bond lengths and high Si occupancy in T site. It is concluded that the “Ca-minimum” in the clinopyroxene structure is regarded as the lowest value at which the charge balance requirements are satisfied in a C2/c clinopyroxene structure.

Introduction

Clinopyroxene crystal structure is generally a sensitive indicator of the physico-chemical conditions of equilibration specific to the host rock suite (Dal Negro et al. 1989). A notable feature of clinopyroxene crystal chemistry is that intracrystalline variations depend on either the crystallization environment (e.g., pressure, temperature, oxygen fugacity) or the structural constraints that a specific site induces on the geometry of the other sites.

This paper discusses crystal chemical analyses of clinopyroxenes crystallized from magmas ranging in composition from basalt to pantellerite. The main objective here is to describe the relationships in clinopyroxene site geometry with melt composition variability and structur-

al constraints, particularly those bearing on the “Ca-pyroxene minimum” typical of tholeiitic suites.

Petrological notes

The clinopyroxenes investigated in this study were from volcanic rocks of the Bosetti Complex (Main Ethiopian Rift) whose compositions range from transitional basalts to pantellerites. The evolution from basalts to peralkaline rhyolites occurred through fractional crystallization under quartz – fayalite – magnetite (QFM) f_{O_2} buffer conditions, with the exception of the pantelleritic stage which was characterized by the absence of olivine and Fe–Ti oxides. Liquidus temperatures (Nathan and Van Kirk 1978) range from 1220°C (transitional basalt) to 1065°C (pantellerite) and are consistent with those calculated from mineral compositions (Brotzu et al. 1980; Ganeo 1982).

The selected rock types (cf. Appendix) are typical of basalt – trachyte – pantellerite suites. Whole rock and mineral compositions were presented by Brotzu et al. (1980), and mineral assemblages and some chemical and normative parameters are found in the Appendix.

Mineral separation and analytical methods

The analyzed clinopyroxenes were selected under a petrographic microscope from rock sections about 100 µm thick. Only optically homogeneous crystal fragments, usually from the cores of microphenocrysts, were chosen for X-ray diffraction and microanalysis. X-ray diffraction data were obtained with a computer-controlled SIEMENS AED II four-circle diffractometer with MoK α radiation monochromatized by a flat graphite crystal, using techniques and procedures given by Dal Negro et al. (1982). The crystal fragments used in the X-ray diffraction studies were subsequently mounted on glass slides and polished for electron microprobe analysis with an ETEC-AUTOSCAN-AUTOSPEC system operating at 15 KV. The ORTEC MAGIC IV version of the MAGIC program (Colby 1972) was used to convert X-ray counts into an oxide analysis. Results are considered to be accurate within 2–5% for major elements and about 9% for minor elements.

Chemical composition and crystal chemistry

The chemical compositions and crystal structural parameters of the clinopyroxene samples are presented in Tables 1 and 2, respectively.

Table 1. Chemical composition and site occupancy of Boseti clinopyroxenes on the basis of six oxygens (see text): $R^{3+} = (Al^{VI} + Ti^{4+} + Cr^{3+})$

	1	2	3	4	5	6	7	8	9	10	11	12	13	14	15	16	17	18
SiO ₂	50.32	51.35	50.61	48.97	50.82	51.55	52.19	51.17	51.00	49.61	48.38	47.60	48.84	48.14	48.00	48.24	49.30	47.83
TiO ₂	1.24	1.36	1.61	1.66	0.67	0.63	0.37	0.41	0.28	0.34	0.37	0.48	0.44	0.64	0.07	0.58	0.19	0.39
Al ₂ O ₃	4.57	1.52	3.49	4.42	1.34	0.78	0.81	0.94	0.37	—	0.14	0.31	0.13	0.25	0.22	0.12	0.50	0.04
FeO _t	7.31	9.74	9.23	8.41	14.50	13.49	12.60	14.43	20.40	23.12	25.06	28.90	22.70	28.90	28.30	28.54	28.18	29.11
MnO	—	0.13	0.32	0.06	0.84	1.16	1.09	1.20	1.74	2.24	1.63	1.77	1.84	1.63	1.61	1.54	1.18	1.53
MgO	14.20	13.75	15.45	13.44	10.71	13.94	13.08	12.48	7.50	4.79	2.72	0.10	4.65	0.52	0.15	0.22	0.02	0.18
CaO	20.77	22.00	19.13	20.74	19.60	17.64	18.99	17.54	18.50	19.42	19.63	19.30	18.72	19.62	19.00	18.68	15.26	16.62
Na ₂ O	0.44	0.15	0.07	0.50	0.49	0.23	0.53	0.59	0.61	0.47	0.54	0.73	0.43	0.31	1.14	1.07	4.27	2.00
Cr ₂ O ₃	0.43	—	0.03	0.03	0.08	—	—	—	—	—	—	—	—	—	0.05	—	—	
Sum	99.28	100.00	99.94	98.23	99.05	99.42	99.66	98.76	100.40	99.99	98.47	99.19	97.75	100.01	98.49	99.04	98.90	97.70
Si	1.875	1.933	1.881	1.852	1.960	1.962	1.975	1.964	1.993	2.000	1.993	1.985	1.996	1.988	1.989	2.000	1.998	1.998
Al ^{IV}	0.125	0.067	0.119	0.148	0.040	0.038	0.025	0.036	0.007	—	0.007	0.015	0.004	0.012	0.011	—	0.002	0.002
Sum	2.000	2.000	2.000	2.000	2.000	2.000	2.000	2.000	2.000	2.000	2.000	2.000	2.000	2.000	2.000	2.000	2.000	
Al ^{VI}	0.075	—	0.034	0.049	0.021	—	—	0.007	0.008	—	—	—	0.006	—	—	—	—	—
Fe ²⁺	0.157	0.167	0.129	0.143	0.342	0.190	0.241	0.262	0.546	0.680	0.828	0.966	0.695	0.948	0.909	0.950	0.690	0.837
Fe ³⁺	—	0.031	0.010	0.030	—	0.041	—	0.019	—	0.017	—	0.013	0.001	—	0.061	0.010	0.304	0.139
Mg	0.720	0.764	0.781	0.730	0.616	0.751	0.738	0.700	0.438	0.293	0.160	0.006	0.284	0.032	0.009	0.020	—	0.012
Ti ⁴⁺	0.035	0.038	0.045	0.047	0.019	0.018	0.011	0.012	0.008	0.010	0.012	0.015	0.014	0.020	0.021	0.018	0.006	0.012
Cr	0.013	—	0.001	0.001	0.002	—	—	—	—	—	—	—	—	—	0.002	—	—	
Sum	1.000	1.000	1.000	1.000	1.000	1.000	1.000	1.000	1.000	1.000	1.000	1.000	1.000	1.000	1.000	1.000	1.000	
Ca	0.829	8.864	0.762	0.841	0.810	0.720	0.768	0.721	0.775	0.810	0.840	0.849	0.821	0.868	0.843	0.850	0.646	0.744
Na	0.032	0.011	0.005	0.037	0.037	0.017	0.039	0.044	0.046	0.035	0.038	0.042	0.034	0.025	0.037	0.048	0.300	0.162
Fe ²⁺	0.071	0.107	0.148	0.092	0.126	0.187	0.158	0.182	0.121	0.079	0.064	0.047	0.081	0.050	0.064	0.048	0.013	0.040
Mg ²⁺	0.068	0.014	0.075	0.028	—	0.039	—	0.014	—	—	—	—	—	—	—	—	—	
Mn ²⁺	—	0.004	0.010	0.002	0.027	0.037	0.035	0.039	0.058	0.076	0.058	0.062	0.064	0.057	0.056	0.054	0.041	0.054
Sum	1.000	1.000	1.000	1.000	1.000	1.000	1.000	1.000	1.000	1.000	1.000	1.000	1.000	1.000	1.000	1.000	1.000	
R ³⁺	0.123	0.069	0.090	0.127	0.042	0.059	0.011	0.038	0.016	0.027	0.012	0.028	0.021	0.020	0.082	0.030	0.310	0.151

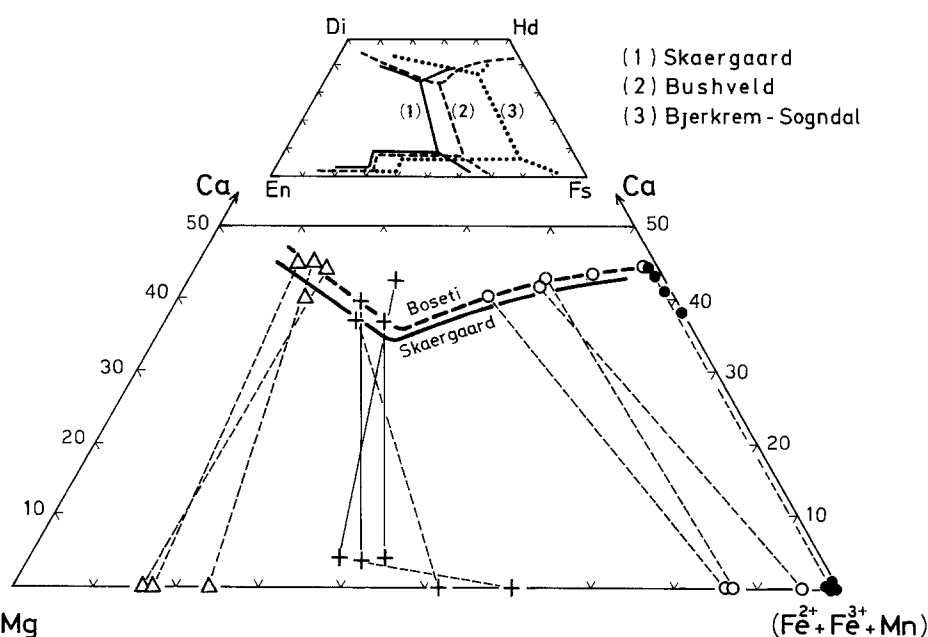


Fig. 1. Ca–Mg–(Fe²⁺ + Fe³⁺ + Mn) plot of the Boseti clinopyroxenes (Cpx) and coexisting orthopyroxene and olivine. Clinopyroxene evolutionary trends in subalkaline basic intrusions (Campbell and Nolan 1974) are shown for comparison. Triangles = basaltic rocks; crosses = intermediate rocks; circles = comendites; solid circles = pantellerites

Table 2. Polyhedral geometry of Boseti clinopyroxenes: ($\sigma^2(T)$): variance of the tetrahedral angles; Robinson et al. (1971); ($\lambda(T)$): mean tetrahedral quadratic elongation parameter; Robinson et al. 1971

	1	2	3	4	5	6	7	8	9
a (Å)	9.743 (1)	9.754 (1)	9.742 (1)	9.749 (1)	9.765 (1)	9.745 (1)	9.753 (1)	9.752 (1)	9.782 (1)
b (Å)	8.900 (1)	8.924 (1)	8.906 (1)	8.901 (1)	8.948 (1)	8.934 (1)	8.941 (1)	8.944 (1)	8.976 (1)
c (Å)	5.269 (1)	5.262 (1)	5.267 (1)	5.273 (1)	5.259 (1)	5.256 (1)	5.256 (1)	5.254 (1)	5.255 (1)
β (°)	106.21 (1)	106.16 (1)	106.30 (1)	106.21 (1)	106.11 (1)	106.48 (1)	106.32 (1)	106.36 (1)	105.92 (1)
v (Å ³)	438.72	439.93	438.61	439.38	441.47	438.80	439.86	439.71	443.71
N _{obs.}	562	524	577	573	560	541	513	544	565
R _{obs}	2.0	2.4	2.7	1.8	2.4	2.5	2.9	2.9	2.3
<i>M1 site</i>									
M1–O2	2.034 (2)	2.048 (2)	2.041 (2)	2.035 (2)	2.057 (2)	2.049 (2)	2.055 (2)	2.054 (2)	2.068 (2)
M1–O1A2	2.056 (1)	2.063 (2)	2.056 (2)	2.057 (1)	2.077 (2)	2.064 (2)	2.069 (2)	2.069 (2)	2.093 (2)
M1–O1A1	2.129 (1)	2.138 (2)	2.134 (2)	2.131 (1)	2.143 (2)	2.146 (2)	2.143 (2)	2.148 (2)	2.154 (2)
mean	2.073	2.083	2.077	2.074	2.092	2.086	2.089	2.090	2.105
V (M1)	11.78	11.96	11.85	11.80	12.12	12.02	12.07	12.10	12.36
<i>M2 site</i>									
M2–O2	2.313 (2)	2.305 (2)	2.298 (2)	2.318 (1)	2.292 (2)	2.260 (2)	2.278 (2)	2.267 (2)	2.292 (2)
M2–O1	2.343 (1)	2.337 (2)	2.330 (2)	2.346 (1)	2.326 (2)	2.302 (2)	2.313 (2)	2.307 (2)	2.322 (2)
M2–O3C1	2.578 (2)	2.596 (2)	2.591 (2)	2.578 (1)	2.610 (2)	2.627 (2)	2.624 (2)	2.626 (2)	2.629 (2)
M2–O3C2	2.731 (2)	2.745 (2)	2.745 (2)	2.728 (1)	2.759 (2)	2.780 (2)	2.768 (2)	2.775 (2)	2.764 (2)
mean	2.491	2.496	2.491	2.493	2.497	2.492	2.496	2.494	2.502
V (M2)	25.51	25.60	25.43	25.56	25.57	25.32	25.48	25.40	25.70
<i>T site</i>									
T–O2	1.599 (2)	1.592 (2)	1.592 (2)	1.599 (1)	1.591 (2)	1.591 (2)	1.587 (2)	1.592 (2)	1.586 (2)
T–O1	1.617 (1)	1.610 (2)	1.616 (2)	1.617 (1)	1.607 (2)	1.610 (2)	1.607 (2)	1.606 (2)	1.605 (2)
T–O3A1	1.666 (2)	1.661 (2)	1.665 (2)	1.667 (1)	1.663 (2)	1.660 (2)	1.663 (2)	1.661 (2)	1.664 (2)
T–O3A2	1.683 (2)	1.685 (2)	1.680 (2)	1.686 (1)	1.684 (2)	1.675 (2)	1.678 (2)	1.675 (2)	1.677 (2)
T–O _{n,brg.}	1.608	1.601	1.604	1.608	1.599	1.601	1.597	1.599	1.596
T–O _{brg.}	1.675	1.673	1.673	1.677	1.674	1.668	1.671	1.668	1.671
V (T)	2.250	2.233	2.239	2.255	2.230	2.222	2.221	2.221	2.219
$\sigma^2(T)$	24.28	24.04	23.91	24.00	24.40	22.42	23.01	22.44	21.97
$\lambda(T)$	1.0057	1.0057	1.0057	1.0057	1.0058	1.0053	1.0054	1.0053	1.0052

In the conventional Ca–Mg–Fe diagram (Fig. 1), the Boseti clinopyroxene shows a trend which parallels that of the Skaergaard suite. In general, most Boseti rock types are characterized by clinopyroxene and olivine (Fa_{16–96}), except for trachytes 5, 7, and 8, in which clinopyroxene is associated with orthopyroxene and aenigmatite-bearing pantellerites (17, 18) where olivine and magnetite are absent. The clinopyroxene of these rock types has high Fe³⁺ content (0.139–0.304 atoms formula unit) and Na (0.162–0.300 a.f.u.). The Boseti clinopyroxene trend (Fig. 1) has a Ca-minimum, like those shown by clinopyroxene suites of several tholeiitic intrusions (e.g., inset of Fig. 1). The latter intrusions show clinopyroxene trends with Ca-minima with quite different Mg/Fe ratios (0.5–1.6), but similar Ca content (0.65–0.75 a.f.u.).

M1 polyhedron

The geometry of the M1 site of the Boseti clinopyroxene appears to be particularly influenced by Fe²⁺ (M1), which ranges from 0.13 to 0.97 a.f.u. A minor role is played by R³⁺ cations (Fe³⁺, Cr³⁺, Al³⁺, Ti⁴⁺) because of their low concentration (average 0.07 a.f.u.).

As documented by Dal Negro et al. (1982), the shortening of the M1–O2 bond length is well correlated with increasing R³⁺ content, implying positive correlations between Fe²⁺ and Mg content and longer M1–O1, A1 and M1–O1, A2 bond distances. The best linear correlation ($r=0.998$) is found between Fe²⁺ and M1–O1, A2 (Fig. 2), while that of M1–O1, A1 shows significant deviations from linearity (inset in Fig. 2). These deviations are observed in the clinopyroxenes of basalts 1, 3, and 4 and pantellerites 15, 17 and 18 all of which are characterized by high R³⁺ content (0.08–0.31 a.f.u.). The substitution of R³⁺ on M1 causes an important volume reduction, for similar Fe²⁺ (M1) content (Fig. 3).

The linear relationships between Fe²⁺ (M1) content and $\langle M1–O \rangle$ bond distances, particularly for clinopyroxene with R³⁺ lower than 0.06 a.f.u., permit the calculation of $\langle M1–O \rangle$ bond lengths for M1 site fully occupied by Fe²⁺. Such calculations give the following values (Å):

M1–O2 = 2.080 ($r=0.982$), M1–O1, A2 = 2.131 ($r=0.998$) and M1–O1, A1 = 2.166 ($r=0.952$), giving a mean $\langle M1–O \rangle = 2.126$. The $\langle M1–O \rangle$ mean value of 2.126 Å for clinopyroxene corresponds exactly to that (2.126 Å) reported by Ungaretti (1981) for metamorphic

Table 2 (continued)

	10	11	12	13	14	15	16	17	18
a (Å)	9.796 (1)	9.814 (1)	9.827 (1)	9.800 (1)	9.828 (1)	9.819 (1)	9.822 (1)	9.778 (1)	9.800 (1)
b (Å)	8.989 (1)	9.002 (1)	9.015 (1)	8.988 (1)	9.012 (1)	9.004 (1)	9.008 (1)	8.955 (1)	8.981 (1)
c (Å)	5.256 (1)	5.256 (1)	5.256 (1)	5.256 (1)	5.256 (1)	5.258 (1)	5.257 (1)	5.267 (1)	5.264 (1)
β (°)	105.75 (1)	105.44 (1)	105.30 (1)	105.67 (1)	105.30 (1)	105.40 (1)	105.31 (1)	105.83 (1)	105.67 (1)
V (Å ³)	445.45	447.59	449.13	445.75	449.02	448.17	448.61	443.70	446.09
N _{obs.}	521	528	532	539	542	540	523	537	537
R _{obs}	2.1	1.7	2.4	2.4	2.0	3.7	1.6	1.7	3.0
<i>M1 site</i>									
M1–O2	2.071 (2)	2.076 (2)	2.077 (2)	2.071 (2)	2.079 (2)	2.070 (3)	2.076 (1)	2.042 (1)	2.057 (3)
M1–O1A2	2.103 (2)	2.117 (2)	2.126 (2)	2.105 (2)	2.125 (2)	2.123 (3)	2.126 (1)	2.101 (1)	2.118 (2)
M1–O1A1	2.157 (2)	2.161 (2)	2.162 (2)	2.153 (2)	2.165 (2)	2.159 (3)	2.161 (1)	2.144 (1)	2.155 (2)
mean	2.110	2.118	2.122	2.110	2.123	2.117	2.121	2.096	2.110
V (M1)	12.45	12.59	12.66	12.44	12.68	12.58	12.64	12.18	12.44
<i>M2 site</i>									
M2–O2	2.295 (2)	2.311 (2)	2.319 (2)	2.303 (2)	2.318 (2)	2.324 (3)	2.327 (1)	2.348 (1)	2.329 (3)
M2–O1	2.326 (2)	2.336 (2)	2.342 (2)	2.335 (2)	2.340 (2)	2.345 (3)	2.348 (1)	2.364 (2)	2.350 (3)
M2–O3C1	2.629 (2)	2.629 (2)	2.635 (2)	2.627 (2)	2.632 (2)	2.623 (2)	2.624 (1)	2.567 (2)	2.604 (3)
M2–O3C2	2.764 (2)	2.750 (2)	2.752 (2)	2.755 (2)	2.752 (2)	2.757 (3)	2.749 (1)	2.770 (2)	2.768 (2)
mean	2.504	2.507	2.512	2.505	2.511	2.512	2.512	2.512	2.513
V (M2)	25.77	25.90	26.07	25.83	26.04	26.09	26.10	26.15	26.13
<i>T site</i>									
T–O2	1.590 (2)	1.586 (2)	1.587 (2)	1.589 (2)	1.588 (2)	1.588 (3)	1.588 (2)	1.589 (2)	1.589 (3)
T–O1	1.605 (2)	1.604 (2)	1.605 (2)	1.605 (2)	1.605 (2)	1.605 (3)	1.603 (2)	1.609 (1)	1.602 (2)
T–O3A1	1.660 (2)	1.664 (2)	1.661 (2)	1.665 (2)	1.660 (2)	1.659 (3)	1.664 (2)	1.654 (1)	1.656 (2)
T–O3A2	1.680 (2)	1.681 (2)	1.682 (2)	1.678 (2)	1.683 (2)	1.683 (3)	1.678 (2)	1.677 (1)	1.680 (2)
T–O _{n,brg.}	1.598	1.595	1.596	1.597	1.597	1.597	1.596	1.599	1.596
T–O _{brg.}	1.670	1.673	1.672	1.672	1.672	1.671	1.671	1.666	1.668
V (T)	2.222	2.222	2.223	2.223	2.224	2.222	2.221	2.217	2.215
σ^2 (T)	22.14	22.72	22.20	23.12	21.84	21.71	21.18	20.02	20.52
λ (T)	1.0053	1.0054	1.0053	1.0055	1.0052	1.0052	1.0051	1.0048	1.0049

amphiboles with M1 and M3 sites fully occupied by Fe²⁺. For natural clinopyroxene, the <M1–O> mean bond distance of 2.126 Å is close to that (2.130 Å) obtained by Cameron et al. (1973) for a synthetic hedenbergite.

M2 polyhedron

M2 is the most irregular site since it coordinates eight oxygens at very variable bond lengths. The shortest bond distances (M2–O2=2.26–2.35 Å and M2–O1=2.30–2.37 Å) of the Bosetti clinopyroxene correlate linearly with (Ca+Na) increase (Fig. 4A). The average decrease of M2–O2 and M2–O1 bond distances with the entry of Fe²⁺, Mg and Mn substituting for (Ca+Na) is 3.4%. In contrast, the longest bond lengths (M2–O3, C1=2.57–2.63 Å and M2–O3, C2=2.73–2.78 Å) generally correlate negatively with (Ca+Na) increase; the best linear correlation is observed for the M2–O3, C2 bond distance.

The clinopyroxene of the aenigmatite-bearing pantellerites (17, 18) is distinct from that of the other acid rock-types due to its high Na content which causes a significant shortening of M2–O3, C1 and concurrent lengthening of M2–O3, C2 distances in order to provide the charge balance of oxygen O3. In general, the longest

<M2–O3> bond distances of clipyroxenes from acid volcanics are longer than those of clinopyroxenes from basalts (Dal Negro et al. 1982; present study), while the contrary tends to occur for the shortest M2–O2 and M2–O1 bond lengths (Fig. 4). These differences in geometrical variations are due to the comparatively high Al^{IV} and low Fe²⁺ (M1) content in clinopyroxenes from basalts with respect to that from acid volcanics. Note that the latter clinopyroxene has the T site virtually filled by Si⁴⁺ (higher than 1.96 a.f.u.), which greatly contributes to the charge balance of the oxygen O3 and allows lengthening of <M2–O3> bond distances (see below).

T polyhedron

Typically, the Bosetti clinopyroxenes from acid rock types show a near-full occupancy of T site by Si⁴⁺. As documented by Carbonin et al. (1984), high Si⁴⁺ content in clinopyroxene from acid volcanics is essentially related to high Fe²⁺ content in the M1 site rather than to the alkaline or subalkaline nature of the magmas (e.g., phonolite or rhyolite). The increase of Fe²⁺ in the M1 site causes lengthening of M1–O bond distances and this requires shortening of T–O1 and T–O2 bond lengths and Si enrichment. The trachytic-rhyolitic clinopyroxene from Bosetti, which is characterized by high

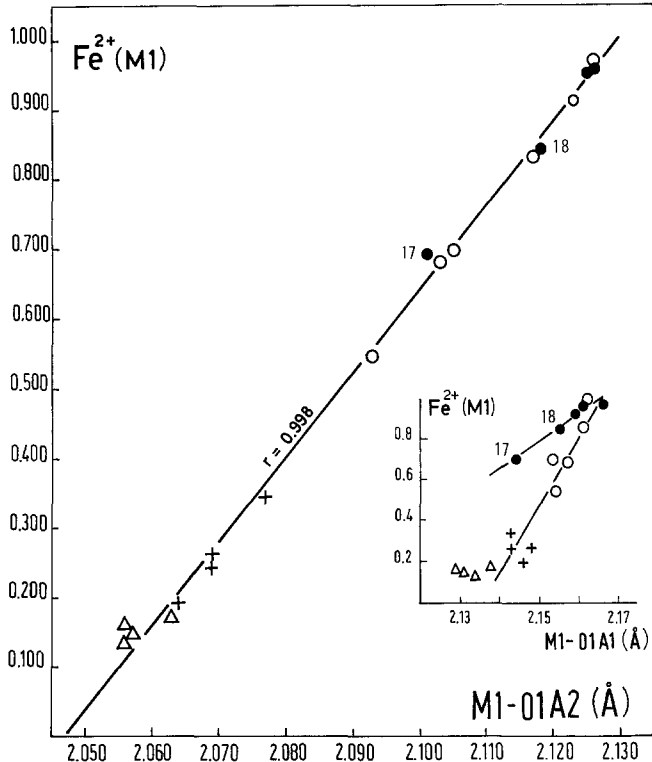


Fig. 2. Fe^{2+} (M1) (a.f.u.) vs $\text{M1}-\text{O}1\text{A}2$ bond length plot. The positive correlation in the Bosetti clinopyroxenes has a linear coefficient of 0.998, whereas the plot of Fe^{2+} (M1) vs $\text{M1}-\text{O}1\text{A}1$ bond length (inset) shows a deviation from linearity in pantellerite clinopyroxenes. Symbols as in Fig. 1

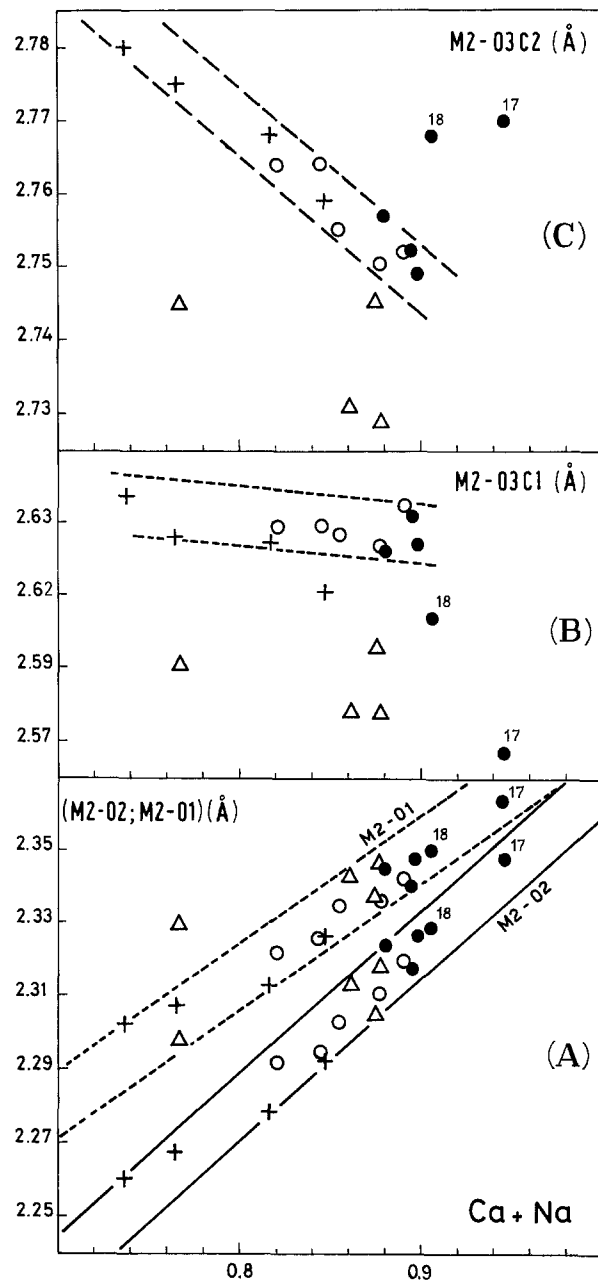


Fig. 4A-C. Plot of $\text{Ca} + \text{Na}$ (a.f.u.) vs $\langle \text{M}2-\text{O} \rangle$ bond lengths in Bosetti clinopyroxenes: positive correlations for $\text{M}2-\text{O}2$ and $\text{M}2-\text{O}1$ (A), negative for $\text{M}2-\text{O}3\text{C}1$ and $\text{M}2-\text{O}3\text{C}2$ bond lengths (B) and (C). Note shortening and lengthening of $\text{M}2-\text{O}3\text{C}1$ and $\text{M}2-\text{O}3\text{C}2$ respectively, in pantellerite clinopyroxenes 17, 18 caused by high Na content. Symbols as in Fig. 1

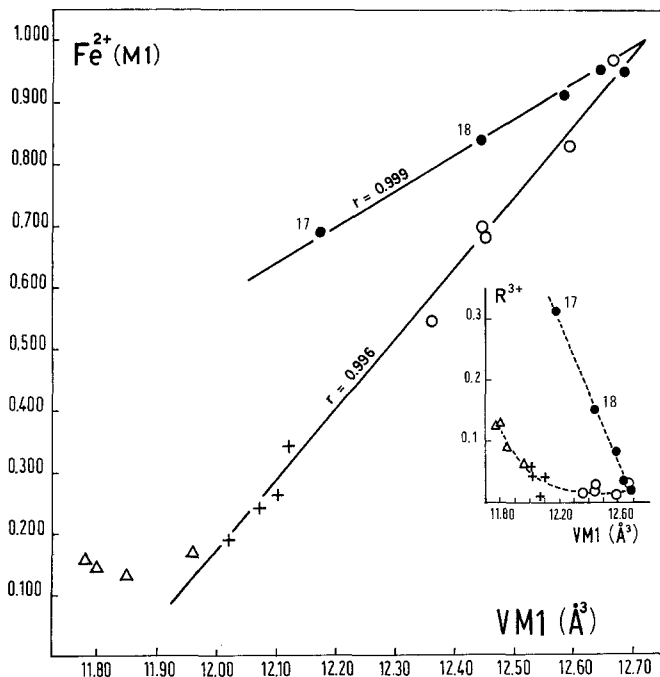


Fig. 3. Relationships between $\text{V}\text{M}1$ and Fe^{2+} (M1) content (atoms per formula unit) in Bosetti clinopyroxenes. Pantellerite clinopyroxenes show relevant volume reduction relative to others with same Fe^{2+} (M1) because of significant R^{3+} (M1) (see inset). Symbols as in Fig. 1

Fe^{2+} in the M1 site (ca. 0.20–0.95 a.f.u., Table 1) and large $\text{VM}1$ ($> 12.0 \text{ \AA}^3$), conforms to this picture.

A striking feature of the Bosetti clinopyroxene with Si contents higher than 1.960 a.f.u., is the large variation of λ (T) and σ^2 (T) distortion parameters (Robinson et al. 1971). Note that in Fig. 5 the smallest degrees of distortion with very short $\langle \text{T}-\text{O} \rangle_{\text{brg}}$ bond lengths (1.665 and 1.668 Å, respectively) occur for clinopyroxene with the highest Na content (n. 17, 18) which gives a lower charge contribution to oxygen O3 than that of a corresponding amount of Ca.

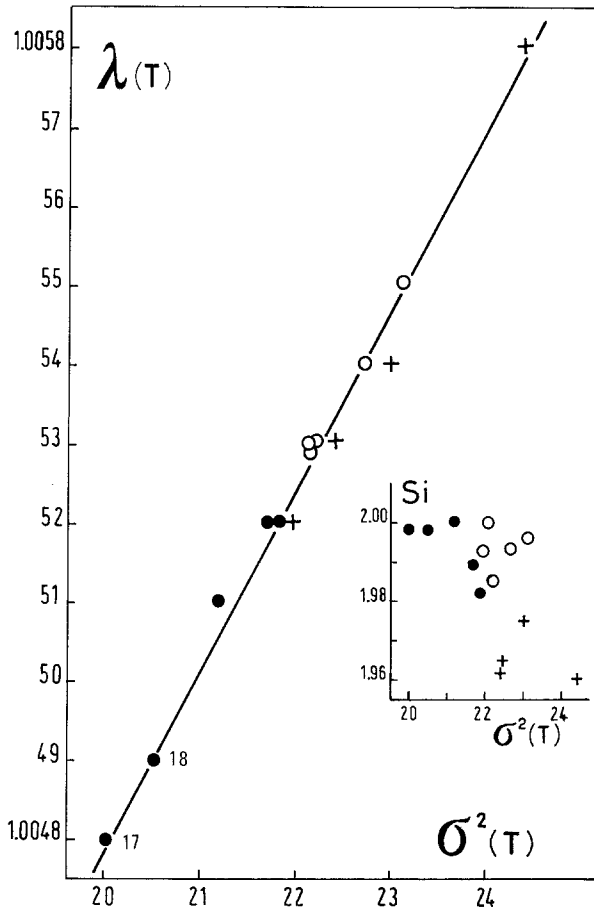


Fig. 5. Plot of σ^2 (T) vs λ (T) (Robinson et al. 1971) in Bosetti clinopyroxenes with Si > 1.96 a.f.u. Smallest distortion parameters refer to pantellerite clinopyroxenes 17, 18 with very short $\langle T-O \rangle_{\text{brg}}$ bond lengths and high Na content

Discussion

The compositional variations of the Bosetti clinopyroxenes are shown in Fig. 6 in which cation abundances (a.f.u.) are plotted against the Mg/Mg + Fe²⁺ ratio (mg) of the clinopyroxene. In general, the progressive Cpx-mg decrease is associated with clear trends in the different cations concentrations, indicating continuous crystalchemical response of the clinopyroxene to compositional variations in the source melt. This is illustrated, for example, by the regular Mg (M1) decrease, and Fe²⁺ (M1) and Mn increases for clinopyroxene crystallized from basalt to peralkaline acid magmas. Thus, Fe²⁺ (M1) can be taken as a monitor of the evolutionary degree from basalt to pantellerite, for the studied suite. It is important to note that the sharp decrease in Fe²⁺ (M1) and the concurrent sharp increase in Fe³⁺ and Na in the aenigmatite-bearing pantellerites reflect changed f_{O₂} conditions. In the latter rock-types, clinopyroxene crystallized under unbuffered conditions (the "no-oxide" field of Carmichael et al. 1974) in contrast to the clinopyroxene which crystallized from the other peralkaline rocks that are characterized by olivine and magnetite (i.e., QFM buffer).

The transition from basalt to trachyte Cpx is characterized by a Ca decrease (0.86 to 0.72 a.f.u.) associated

with concurrent Mg (M2) exhaustion, while Fe²⁺ (M1), Fe²⁺ (M2) and Mn (M2) increase. Ca decrease is probably related to high activity of low-Ca pyroxene component in Cpx, and the sharp Si increase (over 1.955 a.f.u.) reflects the higher SiO₂ activity in the trachytic melt. High Si content causes a reduction in $\langle T-O \rangle_{\text{non-brg}}$ and a concurrent Fe²⁺ (M1) increase (i.e., lengthening of M1-O1 and M1-O2 bond distances).

The transition from trachyte to pantellerite Cpx (Fig. 6) is characterized by a distinct Ca increase (up to 0.87 a.f.u.), associated with significant Fe²⁺ (M2) depletion, with simultaneous Fe²⁺ (M1) increase. The Bosetti-Cpx suite thus shows a Ca-minimum, similar to those of Cpx suites crystallized from basalt intrusions that have evolved under reducing conditions (cf. Campbell and Nolan 1974; Fig. 1).

In general, the existence of Ca-pyroxene minima indicates that the stability of clinopyroxene is influenced by the relationships between Ca and $\langle M2-O \rangle$ bond length variations, as shown in Fig. 7. The lowest Ca content (0.607 a.f.u.) occurs in a lunar augite 12052 (Takeda 1972a, b), which is characterized by lamellar exsolutions (c. 2.5% vol.) of pigeonite. It appears that, with decreasing Ca content, there is shortening of the shortest distances (M2-O1, M2-O2) and the lengthening of the longest ones (M2-O3, C1, M2-O3, C2). These variations are important, particularly for M2-O2 and M2-O3, C2 distances which, for Ca = 0.5 a.f.u., would become 2.190 and 2.820 Å, respectively. These bond distances appear, respectively, too short and too long for Ca (M2) coordination in a diopside-like structure. It follows that clinopyroxene with Ca content as low as or lower than 0.5 a.f.u. is unstable; this may explain the "pyroxene miscibility gap" in terms of crystal structure (cf. Takeda 1972a, b; Mellini et al. 1988). Note that M2 site of pigeonite is sevenfold coordinated lacking, relative to Ca-rich clinopyroxene, the bond length corresponding to M2-O3, C2 in the diopside-like structure.

In summary, crystal structure parameters indicate that the minimum Ca content in natural clinopyroxenes, which are a single phase in terms of crystal structure, is about 0.6 a.f.u. (cf. Mellini et al. 1988). This may explain why the "Ca-pyroxene minima" of equilibrium crystallization trend (cf. Muir and Mattey 1982) between 0.6–0.7 a.f.u. Ca, although the Cpx Mg/Fe ratio may show large variations (cf. Fig. 1). It should be stressed that clinopyroxene with microprobe compositions equal to, or lower than, 0.5 a.f.u. Ca (the "Ca-pyroxene minimum" of the metastable trends of Muir and Mattey 1982) does not represent a single phase, as documented by Mellini et al. (1988) with TEM analysis, but is rather composed of fine-scale spinodal-lamellar exsolutions of augite and pigeonite.

The abundant crystal structural data now available on low- and high-pressure clinopyroxenes (Dal Negro et al. 1982, 1984, 1985, 1986, 1989a, b; Carbonin et al. 1984, 1989; present study; Cundari et al. 1986; Cundari and Salviulo 1987; Faraone et al. 1988; Manoli and Molin 1988; Mellini et al. 1988; Secco 1988; Princivalle et al. 1989; Secco et al. 1989) indicate that the chemistry

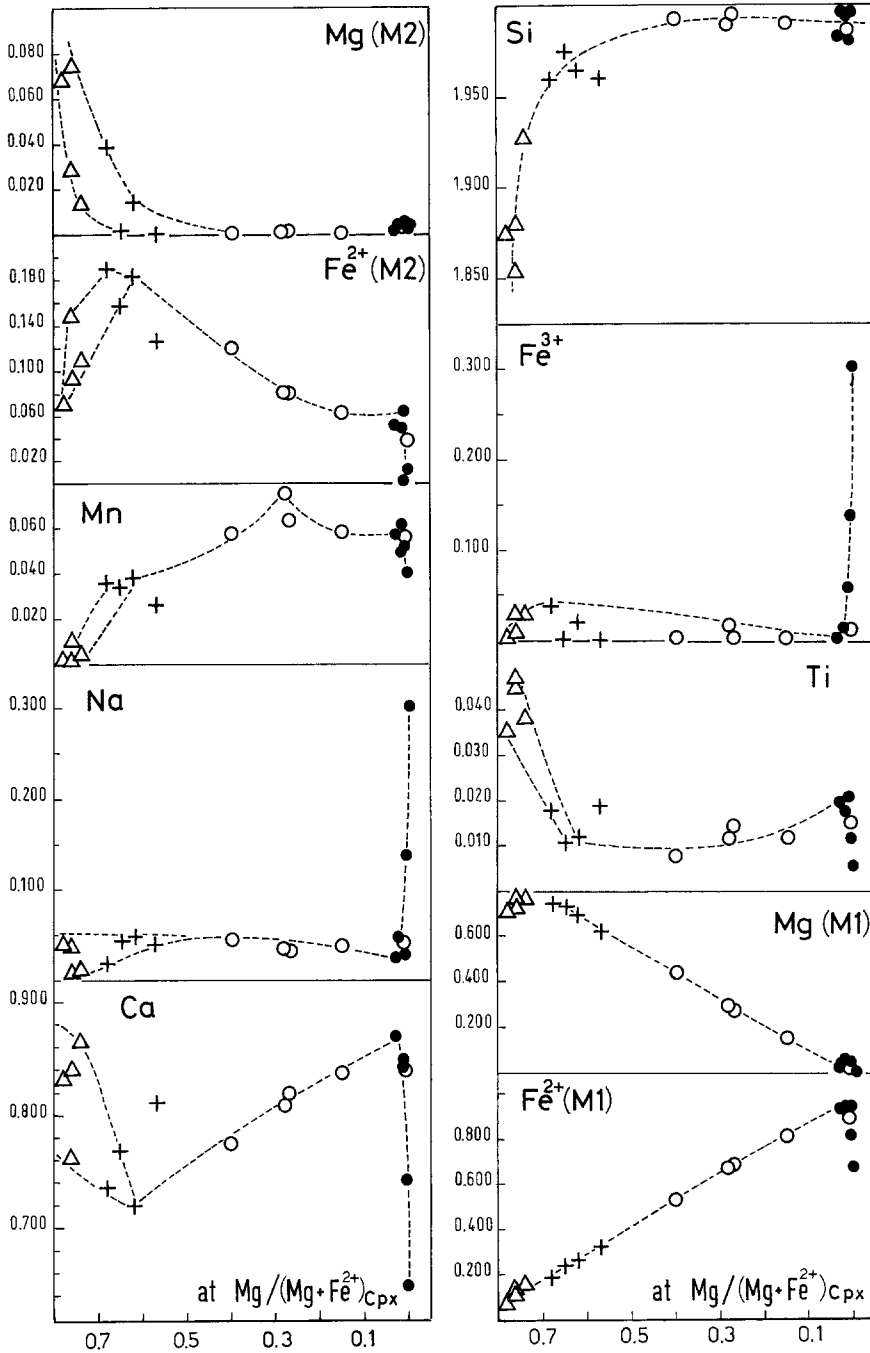


Fig. 6. M2, T, and M1 site occupancy (atoms per formula unit) of Bosetti clinopyroxenes relative to $Mg / (Mg + Fe^{2+})_{cpx}$ ratio of clinopyroxene. Symbols as in Fig. 1

of clinopyroxene crystallizing from basalt magmas is strongly dependent on the structural relationships between T and M2 sites. This means, for example, that if a basalt melt is characterized by high silica activity, the crystallizing clinopyroxene will be characterized by a T site with high Si content (e.g., 1.90 a.f.u.), which in turn requires relatively low Ca content (e.g. 0.60 a.f.u.) in M2 site in order to obtain the charge balance of the O₃ oxygens. In contrast, crystallization of clinopyroxene from intermediate and acid melts is strongly dependent on the geometric variations in the M1 site. For example, large amounts of Fe²⁺ (M1) require large amounts of Si in T site, independently of whether the melt is oversaturated or undersaturated relative to silica. As shown

by Carbonin et al. (1984), this is due to crystal structural constraints, since Fe²⁺ (M1) causes lengthening of M1–O1 and M1–O2 distances and therefore T–O1 and T–O2 bond lengths must become shorter. Note that clinopyroxene from acid volcanics is characterized by high amounts of Si and Ca, which would provide a balance overcharge for the O₃ oxygens. Actually, the charge balance is ensured by lengthening of M2–O₃, C1 and M2–O₃, C2 bond distances relative to those of basalt clinopyroxene (Fig. 7).

Acknowledgements. “Centro di Studio per i Problemi dell’Orogeno delle Alpi Orientali” C.N.R. Padova, and “Ministero della Pubblica Istruzione” are gratefully acknowledged for supporting this research.

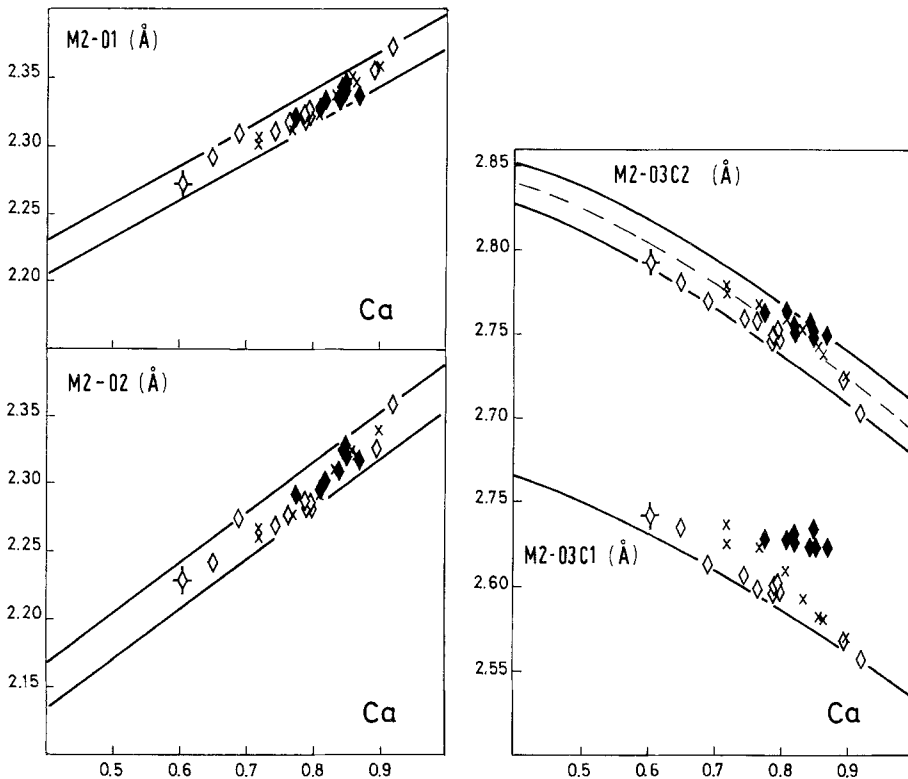


Fig. 7. Plot of Ca content (atoms per formula unit) vs $\langle M2-O \rangle$ bond lengths in clinopyroxenes with $Si > 1.90$ and $Na < 0.05$ a.f.u. relative to basic (diamonds), intermediate (x) and acid (solid diamonds) rock-types. Source data: Takeda (1972a; crossed diamond=lunar sample), Dal Negro et al. (1982), Ganeo (1987) and present study

Appendix

Abbreviations: olivine (ol), plagioclase (pl), Ca-rich pyroxene (cpx), orthopyroxene (opx), opaques (op), alkali feldspar (af), aenigmatite (aeg), magnetite (mt), amphibole (amph), mol. ($Na_2O + K_2O$) / $Al_2O_3 = A.I.$; at $Mg/Mg + Fe^{2+} = M(Fe_2O_3/FeO = 0.15)$. Normative (CIPW) minerals: quartz (Q) hyperstene (Hy), olivine (Ol), acmite (Ac), Na-silicate (Ns).

1 – *M335 (Strongly porphyritic basalt)* Phenocrysts: ol (Fo=83; 2.0%vol), pl (An=63-48; 22.7% vol), cpx (Wo=45; 4.0%vol) and mt (2.4%vol). Groundmass: ol, cpx, pl, op. Q=0.11, Hy=8.5, M=0.442.

2 – *M321 (Transitional basalt)* Phenocrysts and microphenocrysts: ol (Fo=84; 3.2%vol), pl (An=77-55; 9.5%vol), cpx (Wo=44; 0.5%vol) and mt (0.2%vol). Groundmass: ol, cpx, pl, op. Ol=13.3, Hy=0.2, M=0.572.

3 – *M329 (Low-Al hawaiite)* Phenocrysts and microphenocrysts: ol (0.7%vol), pl (An=60-52; 0.6%vol), cpx (Wo=40; 0.2%vol) and mt (1.5%vol). Groundmass: ol, cpx, pl, op. Ol=3.7, Hy=4.8, M=0.372.

4 – *M172 (Low-Al mugearite)* Phenocrysts and microphenocrysts: Ol (Fo=76; 0.6%vol), cpx (Wo=45; 0.5%vol), pl (An=65-50; 3.2%vol), mt (0.1%vol). Groundmass: pl, cpx, op. Q=0.01, Hy=9.4, M=0.360.

5 – *M450 (Mafic trachyte)* Phenocrysts and microphenocrysts: pl (An=36-33; 1.8%vol), cpx (Wo=42; 0.3%vol), opx (En=54; 0.2%vol), mt (2.0%vol). Groundmass: pl, cpx, op, af. Q=0.8, Hy=9.5, M=0.216.

6 – *M421 (Trachyte)* Phenocrysts and microphenocrysts: cpx (Wo=37; 1.7%vol); pl (An=37-17; 0.7%vol), af (Or=13-11; 4.5%vol), ol (Fo=48; 0.7%vol), mt (0.7%vol). Groundmass: pl, cpx, ol, af, op. Q=4.5, Hy=4.3, A.I.=0.96.

7 – *M438 (Trachyte)* Phenocrysts and microphenocrysts: cpx (Wo=40; 1.1%vol), pl (An=25-16; 0.1%vol), af (Or=15-11;

7.6%vol), ol (Fa=57; 0.1%vol), opx (En=56; 0.1%vol) and op (1.9%vol). Groundmass: pl, af, op. Q=8.0, Hy=4.0, A.I.=0.98.

8 – *M526 (Trachyte)* Phenocrysts and microphenocrysts: af (Or=23-15; 7.5%vol), cpx (Wo=37; 1.1%vol), opx (En=48; 0.2%vol), pl (An=18; 0.1%vol) and mt (1.3%vol). Groundmass: af, cpx, Q=7.9, Hy=4.1, A.I.=0.99.

9 – *M531 (Comenditic trachyte)* Phenocrysts and microphenocrysts: ol (Fa=81; 0.7%vol), af (Or=23-16; 8.4%vol), cpx (Wo=40; 0.7%vol), mt (0.5%vol). Groundmass: af, cpx. Q=8.8, Ac=1.8, A.I.=1.02.

10 – *M534 (Comendite)* Phenocrysts and microphenocrysts: ol (0.2%vol) af (Or=24-19; 1.9%vol), cpx (Wo=41; 0.4%vol), mt (0.1%vol). Groundmass: af and cpx. Q=15.8, Ac=2.7, Ns=0.9, A.I.=1.10.

11 – *M535 (Comendite)* Phenocrysts and microphenocrysts: ol (Fa=89; 0.4% vol), af (Or=25-20; 0.8%vol), cpx (Wo=43; 0.4%vol), mt (0.2%vol). Groundmass: af, cpx, op. Q=16.5, Ac=4.5, Ns=1.1, A.I.=1.14.

12 – *M154 (Comendite)* Phenocrysts and microphenocrysts: ol (Fa=92; 0.2%vol), af (Or=20-17; 7.2%vol), cpx (Wo=44; 0.8%vol), mt (0.9%vol), amph (0.1%vol). Groundmass: af, cpx, op. Q=21.0, Ac=2.8. A.I.=1.05.

13 – *M353 (Comendite)* Phenocrysts and microphenocrysts: ol (Fa=88; 0.4%vol), af (Or=20-17; 3.1%vol), cpx (Wo=42; 0.9%vol), mt (0.6%vol). Groundmass: af, cpx, op. Q=12.5, Ac=6.6, Ns=0.03, A.I.=1.11.

14 – *M397 (Pantelleritic trachyte)* Phenocrysts and microphenocrysts: ol (Fa=96; 0.6%vol), af (Or=29-24; 8.7%vol), cpx (Wo=45; 1.2%vol), mt (0.6%vol). Groundmass: af, cpx, op. Q=7.0, Ac=10.7, Ns=0.5, A.I.=1.21.

15 – *M168 (Pantellerite)* Phenocrysts and microphenocrysts: af (Or=30-26; 9.4%vol), ol (Fa=93; 0.8%vol), cpx (Wo=43; 0.8%vol), mt (1.9%vol), aeg(trace). Groundmass: af, cpx. Q=13.3, Ac=8.6, Ns=1.3, A.I.=1.24.

- 16 – *M384 (Pantellerite)* Phenocrysts and microphenocrysts: af (Or = 32; 11.2% vol), ol (Fa = 96; 0.4% vol), cpx (Wo = 44; 0.9% vol), mt (0.4% vol). Groundmass: af, cpx, op. Q = 13.7, Ac = 16.9, A.I. = 1.31.
- 17 – *M395 (Pantellerite)* Phenocrysts and microphenocrysts: af (Or = 36; 0.8% vol), cpx (Wo = 38; 0.4% vol), aeg (0.5% vol). Groundmass: af, cpx, aeg. Q = 25.1, Ac = 7.3, Ns = 6.3, A.I. = 1.72.
- 18 – *M360 (Pantellerite)* Phenocrysts and microphenocrysts: af (Or = 35; 1.8% vol), cpx (Wo = 41; 0.9% vol), aeg (0.2% vol). Groundmass: af. Q = 24.1, Ac = 5.6, Ns = 8.8, A.I. = 2.01.

References

- Brotzu P, Morbidelli L, Piccirillo EM, Traversa G (1980) Volcanological and magmatological evidence of the Boseti volcanic complex (Main Ethiopian Rift). In: Geodynamic evolution of the Afro-Arabian Rift system, vol 47. Acc Naz Lincei, Roma, pp 317–366
- Cameron M, Sueno S, Prewitt CT, Papike JJ (1973) High-temperature crystal chemistry of acmite, diopside, hedenbergite, jadeite, spodumene, and ureyite. *Am Mineral* 58:594–618
- Campbell IH, Nolan J (1974) Factors effecting the stability field of Ca-poor pyroxene and the origin of the Ca-poor minimum in Ca-rich pyroxenes from tholeiitic intrusions. *Contrib Mineral Petro* 48:205–219
- Carbonin S, Dal Negro A, Molin GM, Munno R, Rossi G, Lirer L, Piccirillo EM (1984) Crystal chemistry of Ca-rich pyroxenes from undersaturated to oversaturated trachytic rocks, and their relationships with pyroxenes from basalts. *Lithos* 17:191–202
- Carbonin S, Salviulo G, Munno R, Desiderio M, Dal Negro A (1989) Crystal-chemical examination of natural diopspides: some geometrical indications of Si–Ti tetrahedral substitution. *Mineral Petro* 41:1–10
- Carmichael ISE, Turner FJ, Verhoogen J (1974) Igneous petrology. McGraw-Hill, New York, pp 285–288
- Colby JW (1972) MAGIG IV – a computer program for quantitative electron microprobe analysis. Bell Telephone Laboratories Inc, Allentown, Pennsylvania
- Cundari A, Salviulo G (1987) Clinopyroxenes from Somma – Vesuvius: implications of crystal chemistry and site configuration parameters for studies of magma genesis. *J Petro* 28:727–736
- Cundari A, Dal Negro A, Piccirillo EM, Della Giusta A, Secco L (1986) Intracrystalline relationships in olivine, orthopyroxene, clinopyroxene and spinel from a suite of spinel lherzolite xenoliths from Mt. Noorat, Victoria, Australia. *Contrib Mineral Petro* 94:523–532
- Dal Negro A, Carbonin S, Molin GM, Cundari A, Piccirillo EM (1982) Intracrystalline cation distribution in natural clinopyroxenes of tholeiitic, transitional and alkaline basaltic rocks. In: Saxena SK (ed) Advances in physical geochemistry, vol 2. Springer, New York Berlin Heidelberg, pp 117–150
- Dal Negro A, Carbonin S, Domeneghetti C, Molin GM, Cundari A, Piccirillo EM (1984) Crystal chemistry and evolution of the clinopyroxene in a suite of high pressure ultramafic nodules from the newer volcanics of Victoria, Australia. *Contrib Mineral Petro* 86:221–229
- Dal Negro A, Carbonin S, Salviulo G, Piccirillo EM, Cundari A (1985) Crystal chemistry and site configuration of the clinopyroxene from leucite-bearing rocks and related genetic significance: the Sabatini lavas, Roman Region, Italy. *J Petro* 26:1027–1040
- Dal Negro A, Cundari A, Piccirillo EM, Molin GM, Uliana D (1986) Distinctive crystal chemistry and site configuration of the clinopyroxene from alkali basaltic rocks: the Nyambeni clinopyroxene suite, Kenya. *Contrib Mineral Petro* 92:35–43
- Dai Negro A, Manoli S, Secco L, Piccirillo EM (1989a) Megacrystic clinopyroxenes from Victoria (Australia): crystal chemical comparisons of pyroxenes from high and low pressure regimes. *Eur J Mineral* 1:105–121
- Dal Negro A, Molin GM, Salviulo G, Secco L, Cundari A, Piccirillo EM (1989b) Crystal chemistry of clinopyroxene and its petrogenetic significance: a new approach. In: Boriani A, Bonafe M, Piccardo GB, Vai GB (eds) The lithosphere in Italy: advances in earth science research, vol 80. Acc Naz Lincei, Roma, pp 271–295
- Faraone D, Molin GM, Zanazzi PF (1988) Clinopyroxenes from Vulcano, Aeolian Islands. *Lithos* 22:127–134
- Ganeo S (1982) Studio cristalografico strutturale e cristallochimico di clinopirosseni nella sequenza da basalto a pantellerite del Boseti (Rift Etiopico principale). Thesis, University of Padova, Padova
- Ganeo S (1987) Studio cristalografico-strutturale e cristallochimico di clinopirosseni appartenenti ad una serie tholeitica di arco insulare (Isole Tonga, Pacifico Sud-Ovest). Ph.D. Thesis, University of Padova, Padova
- Manoli S, Molin GM (1988) Crystallographic procedures in the study of experimental rocks: X-ray single-crystal structure refinement of C2/c clinopyroxene from lunar 74275 high-pressure experimental basalt. *Mineral Petro* 39:187–200
- Mellini M, Carbonin S, Dal Negro A, Piccirillo EM (1988) Tholeiitic hypabyssal dykes: how many clinopyroxenes? *Lithos* 22:127–134
- Muir ID, Matthey DA (1982) Pyroxene fractionation in ferrobasalts from the Galapagos spreading centre. *Mineral Mag* 45:193–200
- Nathan HD, Van Kirk OK (1978) A model of magmatic crystallization. *J Petro* 19:66–94
- Princivalle F, Secco L, Demarchi G (1989) Crystal chemistry of a clinopyroxene series in ultrafemic xenoliths from north-eastern Brazil. *Contrib Mineral Petro* 101:131–135
- Robinson K, Gibbs GV, Ribbe PH (1971) Quadratic elongation: a quantitative measure of distortion in coordination polyhedra. *Science* 172:567–570
- Secco L (1988) Crystal-chemistry of high-pressure clinopyroxene from spinel lherzolite nodules: Mts. Leura and Noorat suites, Victoria, Australia. *Mineral Petro* 39:175–185
- Secco L, Carbonin S, Dal Negro A, Mellini M, Piccirillo EM (1989) Crystal chemistry of pyroxenes from basalts and rhyodacites of the Paraná Basin (Brazil). In: Piccirillo EM, Melfi AJ (eds) The Mesozoic flood volcanism of the Paraná Basin. Instituto Astronomico e Geofisico, University of São Paulo, Brazil, pp 93–106
- Takeda H (1972a) Structural studies of rim augite and core pigeonite from lunar rock 12052. *Earth Planet Sci Lett* 15:65–71
- Takeda H (1972b) Crystallographic studies of coexisting aluminan orthopyroxene and augite of high-pressure origin. *J Geophys Res* 77:5798–5811
- Ungaretti L, Mazzi F, Rossi G, Dal Negro A (1981) Crystal-chemical characterization of blue amphiboles. Proceedings of the XI General Meeting of IMA, Novosibirsk, 4–10 September 1978. Rock Forming Minerals, pp 20–45